

Translation Enhancer Improves the Ribosome Liberation from Translation Initiation

Shuntaro Takahashi,^{*,†,‡} Hiroyuki Furusawa,^{†,§} Takuya Ueda,^{||} and Yoshio Okahata^{*,†,§}

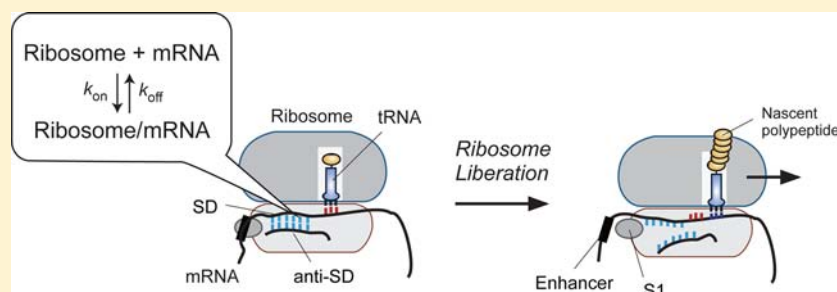
[†]Department of Biomolecular Engineering, Tokyo Institute of Technology, B-53, 4259 Nagatsuda, Midori-ku, Yokohama 226-8501, Japan

[‡]Frontier Institute for Biomolecular Engineering Research (FIBER), Konan University, 7-1-20 Minatojima-minamimachi, Chuo-ku, Kobe 650-0047, Japan

[§]Innovation Flex Course for Frontier Organic Material Systems (iFront), Yamagata University, 4-3-16 Jonan, Yonezawa, Yamagata 992-8510, Japan

^{||}Department of Medical Genome Sciences, Graduate School of Frontier Sciences, University of Tokyo, FSB401, 5-1-5 Kashiwanoha, Kashiwa Chiba 277-8562, Japan

S Supporting Information



ABSTRACT: For translation initiation in bacteria, the Shine–Dalgarno (SD) and anti-SD sequence of the 30S subunit play key roles for specific interactions between ribosomes and mRNAs to determine the exact position of the translation initiation region. However, ribosomes also must dissociate from the translation initiation region to slide toward the downstream sequence during mRNA translation. Translation enhancers upstream of the SD sequences of mRNAs, which likely contribute to a direct interaction with ribosome protein S1, enhance the yields of protein biosynthesis. Nevertheless, the mechanism of the effect of translation enhancers to initiate the translation is still unknown. In this paper, we investigated the effects of the SD and enhancer sequences on the binding kinetics of the 30S ribosomal subunits to mRNAs and their translation efficiencies. mRNAs with both the SD and translation enhancers promoted the amount of protein synthesis but destabilized the interaction between the 30S subunit and mRNA by increasing the dissociation rate constant (k_{off}) of the 30S subunit. Based on a model for kinetic parameters, a 16-fold translation efficiency could be achieved by introducing a tandem repeat of adenine sequences (A20) between the SD and translation enhancer sequences. Considering the results of this study, translation enhancers with an SD sequence regulate ribosomal liberation from translation initiation to determine the translation efficiency of the downstream coding region.

INTRODUCTION

Proteins are translated from the genetic information encoded on mRNAs, where ribosomes decode codons of nucleotide triplets and synthesize polypeptide chains. Translation initiation, when the ribosome is recruited to mRNA, is the rate-limiting event of protein biosynthesis.^{1,2} The 5'-untranslated region (5'-UTR), which is the 5'-upstream sequence of an open reading frame (ORF), is an important region where ribosomes bind to mRNA during translation initiation. For example, the Shine–Dalgarno (SD) sequence, a 3–10-nucleotide purine-rich sequence (A or G) located approximately 10 bases upstream of the start codon (AUG), is the consensus region to initiate the prokaryote translation process (Figure 1).³ Bacterial 30S ribosomal subunits bind to the SD

sequence of mRNAs via the complementary anti-SD sequence at the 3'-terminus of the 16S rRNA of the 30S subunit. Besides the interaction between SD and anti-SD sequences, the amount of protein synthesis is promoted when a pyrimidine-rich region (U or C), called the translation enhancer (Eps), is located immediately upstream of the SD sequence.^{4–12} These translation enhancers likely interact with ribosomal protein S1 on the small subunit of the ribosome.^{11,12} S1 is an RNA-binding protein,^{13–16} and cryo-electron microscopic images support that S1 is located near the SD helix and could interact with the

Received: June 14, 2013

Published: August 8, 2013

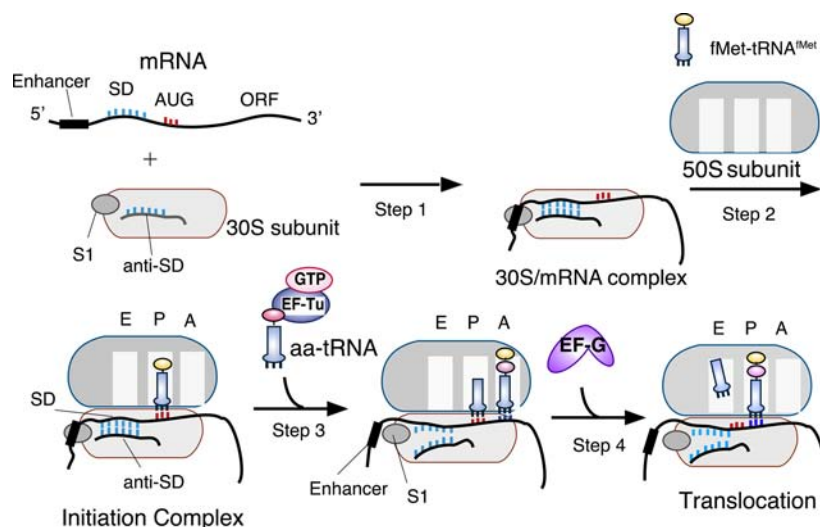


Figure 1. Schematic illustration of the initiation and elongation steps of translation. Step 1: the 30S subunit binds to the SD sequence on mRNA via the interaction between the SD and anti-SD sequences. Step 2: the 50S subunit and fMet-tRNA^{Met} bind to the 30S complex to form the initiation complex. Step 3: EF-Tu delivers the aa-tRNA corresponding to the second codon to the A site. Step 4: EF-G catalyzes the translocation of the 70S ribosome to the next codon. The enhancer sequence is presumed to interact with the S1 protein of the 30S subunit in the 30S/mRNA complex and the initiation complex.

immediate upstream region of the SD sequence, for example, the enhancer sequence.¹⁷

The amount of complex formation between the ribosome and mRNA determines the amount of protein synthesis because a low complementarity of the SD/anti-SD duplex decreases the amount of translated mRNA.¹⁵ However, structural analyses of the initiation complex suggested that the subsequent translation required the release of the SD/anti-SD interaction of the initiation complex to proceed to the elongation phase (Figure 1, Steps 3 and 4).^{18,19} It is plausible that both the association of the SD sequence of mRNA to the anti-SD sequence of the 30S subunit in the initiation complex as well as the dissociation close to translation would be a key step for efficient protein syntheses. To elucidate the mechanism of the control of translation efficiencies, kinetic analyses of ribosome binding to mRNA (the interaction between the SD and anti-SD sequences) are important. Binding kinetic analysis can be used to derive the binding rate constant (k_{on}), the dissociation rate constant (k_{off}), and the equilibrium-binding constant (K_{a}). The purpose of this study is to reveal the relationship between the binding kinetics of the SD/anti-SD sequences in the initiation complex and the amount of protein synthesis by changing SD sequences, introducing several translation enhancers, and changing the spacer length between the SD and enhancer sequences. Both the ribosome dynamics on the mRNAs and their translation efficiencies provide insights into the mechanism of the phase transition from the initiation complex to the elongation process. To determine the kinetics between 30S subunits and mRNAs, we employed the quartz-crystal microbalance (QCM) method,^{20–24} which employs a device (a QCM) to analyze kinetics interactions between biomolecules without any labeling techniques. The translation efficiencies were evaluated using an *Escherichia coli* in vitro translation system, the PURE System. The obtained kinetic parameters suggested that translation enhancers destabilized the initiation complex due to an increased dissociation rate constant (k_{off}). Our results explain how translation enhancers promote downstream gene expression by independent contributions of two different types of inter-

actions: between the SD sequence of the mRNA and the anti-SD sequence of the 30S subunit and between the enhancer sequence of the mRNA and the S1 protein of the 30S subunit.

RESULTS

Effect of SD Sequences on the Binding to the 30S Subunit and Translation Efficiency. The SD sequence is located approximately 7–10 nucleotides upstream of the start codon (e.g., AUG) of prokaryotic mRNA and is composed of a sequence complementary to the 3'-terminus of the 16S rRNA of the 30S ribosomal subunit. This complementarity is one of the factors that determine the efficiency of protein synthesis.¹⁵ We prepared three kinds of biotinylated mRNAs containing different complementarity to the anti-SD sequence of the 30S subunit to examine the binding kinetics of *E. coli* 30S ribosome subunits to each mRNA using the QCM method.²² Biotinylated mRNAs are shown in Figure 2A, where the CanSD mRNA, StrongSD mRNA, and WeakSD mRNA have the SD sequences of CanSD (5'-ACAGGGAGGCA), StrongSD (5'-UAAGGGAGGUG), and WeakSD (5'-ACAGGCGCCA), respectively; the standard sequence is shown and has no enhancer effect (ACAUGGAUUU). The double-underlined and underlined letters indicate complementary nucleotides to the anti-SD sequence and pyrimidine nucleotides (U and C) in the enhancer sequence, respectively. The full sequences of the mRNAs used in this work are summarized in the Supporting Information, Figure S1. Biotinylated mRNAs were immobilized on a NeutrAvidin-coated QCM. After flushing the QCM cell, the 30S subunit was injected into the cell filled with buffer solution to detect the binding kinetics of the 30S subunit to each mRNA using the QCM.

Figure 3A is an illustration of the binding of the 30S subunit to mRNA immobilized on the QCM, and Figure 3B shows typical frequency decreases (mass increases) as a function of time, responding to the addition of the 30S subunits into each mRNA-immobilized QCM. The 30S subunits primarily bound to the StrongSD mRNA and the CanSD mRNA (Figure 3B, curves a and b) and bound less to the WeakSD mRNA (curve

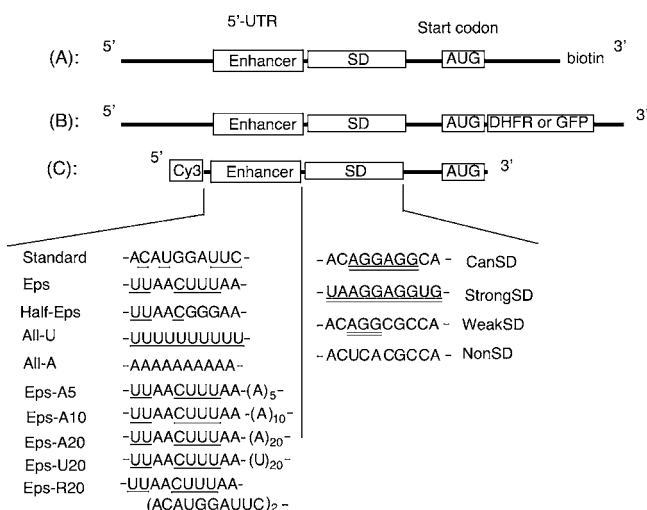


Figure 2. Sequences of mRNAs used in this study. (A) 3'-biotinylated mRNAs, which are designed to immobilize on the NeutrAvidin-covered 27 MHz QCM, (B) mRNAs designed for protein syntheses (DHFR or GFP) using the PURE System, and (C) mRNAs having a fluorescent probe (Cy3) at the 5'-end. Full sequences of mRNAs are described in the Supporting Information (Figure S1). Pyrimidine nucleotides (U and C) are underlined in the enhancer sequences. The double-underlined SD sequence is complementary to the anti-SD sequence of the 30S subunit.

c). The binding affinity is related to the length of the complementary sequence (StrongSD: 10 bases, CanSD: 6 bases, and WeakSD: 3 bases, double-underlined in Figure 2A) of the mRNAs to the anti-SD sequence of the 30S subunit.

To quantify the binding behavior, curves of frequency decreases (mass increases) after the addition of the 30S subunit were fitted by a monoexponential equation to calculate the relaxation time (τ) of the binding of the 30S subunit to mRNA. The kinetic parameters of the binding rate constant (k_{on}), the dissociation rate constant (k_{off}), and the association constant (K_{a}) were obtained from the reciprocal plot of relaxation time (τ) against each different concentration of the added 30S subunit. All parameters determined are summarized in Table 1 (runs 1–3). The association constant (K_{a}) of the 30S subunit was $8.6 \times 10^7 \text{ M}^{-1}$ for the StrongSD mRNA, $6.2 \times 10^7 \text{ M}^{-1}$ for the CanSD mRNA, and $5.0 \times 10^7 \text{ M}^{-1}$ for the WeakSD mRNA. The longer SD sequence conferred a stronger interaction between the 30S subunit and the mRNA. Comparing rate constants, the binding rate constants were similar ($k_{\text{on}} = 1.8 \times 10^5 \text{ M}^{-1} \text{ s}^{-1}$ for the StrongSD mRNA, $k_{\text{on}} = 1.6 \times 10^5 \text{ M}^{-1} \text{ s}^{-1}$ for the CanSD mRNA, and $k_{\text{on}} = 2.0 \times 10^5 \text{ M}^{-1} \text{ s}^{-1}$ for the WeakSD mRNA), but the dissociation rate constants increased with decreasing lengths of the SD sequences ($k_{\text{off}} = 2.1 \times 10^{-3} \text{ s}^{-1}$ for the StrongSD mRNA, $k_{\text{off}} = 2.6 \times 10^{-3} \text{ s}^{-1}$ for the CanSD mRNA, and $k_{\text{off}} = 3.9 \times 10^{-3} \text{ s}^{-1}$ for the WeakSD mRNA). These results indicate that the binding rates of 30S subunits to mRNAs do not depend on the SD sequence of the mRNA; however, the 30S/mRNA complex is easily decomposed with decreasing SD sequence lengths. These results are supported by a previous study of the binding of the 30S subunits to oligo-mRNAs modified with pyrene.²⁵

Translation efficiencies from mRNAs carrying different SD and enhancer sequences were evaluated using a cell-free translation system (PURE System).^{26,27} The dihydrofolate reductase (DHFR)-encoding gene was connected to the SD and enhancer sequences (Figure 2B), and the translation

efficiency of DHFR was evaluated from the UV absorption at 340 nm (50 mM KH_2PO_4 , pH 7.0, 50 mM dihydrofolate (DHF), 60 mM NADPH), as shown in Figure 3E and runs 1–3 in Table 1. As expected, the DHFR expression from the WeakSD mRNA showed a 0.09-fold lower efficiency than that of the CanSD mRNA (1), whereas that of DHFR from the StrongSD mRNA increased slightly (1.4 times). The reactants were also confirmed by SDS-PAGE (Figure S2). These results indicated that the more stable formation of the 30S/mRNA complex showed a greater translation efficiency of the downstream gene expression, as expected.

Effect of Translation Enhancers on Interactions between SD and Anti-SD Sequences. Translation enhancers are located immediately upstream of SD sequences and are primarily composed of pyrimidine bases (U or C). The epsilon sequence (Eps: 5'-UUAACUUUAA), where pyrimidine nucleotides are shown with underlines) is a translation enhancer derived from gene 10 of T7 phage that promotes the expression of downstream genes of any ORFs.^{5,28} Figure 3C shows the typical frequency decreases (mass increases) after the injection of the 30S subunit into the QCM cell, where the CanSD mRNA and the Eps-CanSD mRNA are immobilized. The binding behavior of the 30S subunit to the CanSD sequence decreased when the Eps sequence was introduced (curve b). Although the 30S subunit may interact both with the SD and enhancer sequences on the mRNA, we conclude that the 30S subunit mainly or first binds to the SD sequence as a monoexponential model with 1:1 interactions.²² Binding kinetic parameters are also summarized in Table 1 (runs 2 and 5). Interestingly, the Eps sequence hardly affected the binding rate constants ($k_{\text{on}} = 1.9 \times 10^5 \text{ M}^{-1} \text{ s}^{-1}$ for the Eps-CanSD mRNA and $k_{\text{on}} = 1.6 \times 10^5 \text{ M}^{-1} \text{ s}^{-1}$ for the CanSD mRNA) but increased the dissociation rate constants ($k_{\text{off}} = 4.4 \times 10^{-3} \text{ s}^{-1}$ for the Eps-CanSD mRNA and $k_{\text{off}} = 1.6 \times 10^{-3} \text{ s}^{-1}$ for the CanSD mRNA). The same behavior was observed for the StrongSD mRNA and the Eps-StrongSD mRNA (Table 1, runs 1 and 4). Therefore, the Eps enhancer sequence decreases the stability of the 30S/mRNA complex by increasing the k_{off} values when mRNAs have SD and StrongSD sequences. In contrast, the effect of the Eps sequence on the WeakSD mRNA caused an increase of not only k_{off} value but also k_{on} value (Table 1, runs 3 and 6). Thus, the introduction of the Eps sequence slightly increased the K_{a} value for large k_{on} and k_{off} values. The enhancer sequence increased the stability of the 30S/mRNA complex when the mRNA had only a weak interaction site with the WeakSD sequence. As another confirmation, the adsorption isotherm curve of binding of 30S subunit to mRNA immobilized on a QCM was analyzed (Supporting Information, Figure S3). The affinity of 30S subunit to CanSD mRNA was higher than Eps-CanSD, which agreed well with the results of kinetic analysis.

Furthermore, we evaluated the translation efficiency of DHFR from mRNAs containing Eps sequences. The translation efficiency was in the order of Eps-StrongSD mRNA (4.7) = Eps-CanSD mRNA (4.6) \gg Eps-WeakSD mRNA (0.12). Thus, the translation efficiency from mRNAs containing the Eps sequence increased approximately four times for the CanSD mRNA (1) and StrongSD mRNA (1.4) but not for WeakSD mRNA. The enhancer sequence actually increased the subsequent translation when a stable SD/mRNA complex had formed but did not affect the translation when the SD/mRNA complex was unstable in the presence of the WeakSD sequence. The absolute amount of synthesized protein from Eps-CanSD

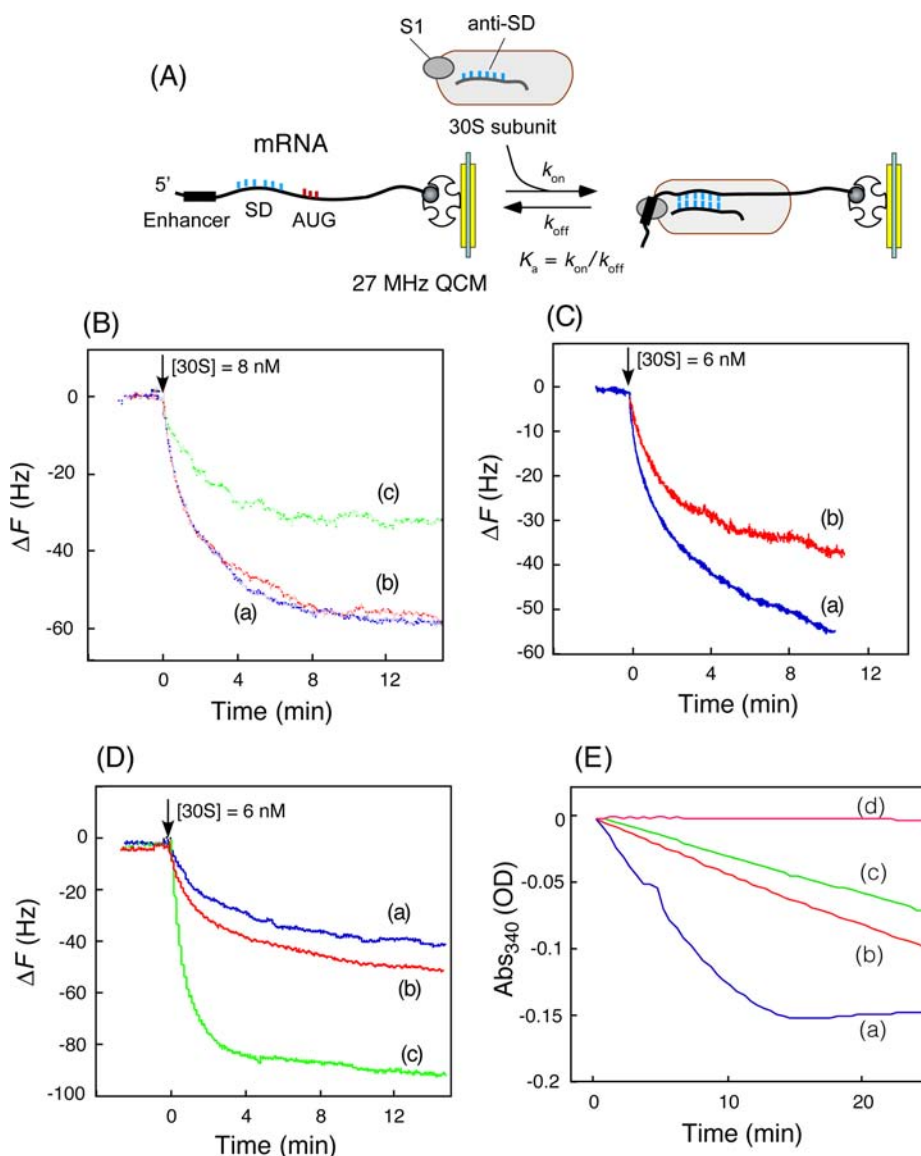


Figure 3. (A) A schematic illustration of bindings of the 30S subunit to biotinylated mRNAs that had been immobilized on NeutrAvidin-covered 27 MHz QCM. (B) Typical time-courses of frequency decreases (mass increases) of (a) the StrongSD mRNA, (b) the CanSD mRNA, and (c) the WeakSD mRNA on the QCM, responding to the addition of 8 nM of the 30S subunit. Arrows indicate the time of the injection of the 30S subunit. (C) Typical time-courses of frequency decreases of (a) the CanSD mRNA and (b) the Eps-CanSD mRNA, responding to the addition of 6 nM of 30S subunit. (D) Typical time-courses of frequency decreases of (a) the CanSD mRNA, (b) the All-A-CanSD mRNA, and (c) the All-U-CanSD mRNA, responding to the addition of 6 nM of 30S subunit. All experiments were performed in the measurement buffer (10 mM HEPES-KOH pH 7.3, 100 mM NH_4Cl , 5 mM $\text{Mg}(\text{OAc})_2$, 0.5 mM CaCl_2) at 25 °C. (E) Typical time-courses of reductions of the absorbance at 340 nm by the reaction of dihydrofolate reductase (DHFR) in the assay solution, indicating the translation amount of DHFR using the PURE System for 1 h at 37 °C. Each initial rate was evaluated as the translated amount of DHFR from (a) the Eps-CanSD mRNA, (b) the StrongSD mRNA, (c) the CanSD mRNA, and (d) the WeakSD mRNA (the corresponding mRNA structures are shown in Figure 2B).

DHFR mRNA was about 0.1 mg/mL, which indicated the standard yield by using the PURE system (Supporting Information of Figure S2). We also confirmed the translation efficiencies by GFP translation (Figure 2B), and similar results were obtained from fluorescent intensities (Supporting Information, Figures S4 and S5).

Effect of the S1 Protein of the 30S Subunit on the Binding of mRNAs. The translation enhancer region directly interacts with ribosomal protein S1 of the 30S subunit. Because S1 strongly binds primarily to the poly pyrimidine of oligo-U and oligo-C,^{29,30} we predicted that the content of U or C nucleotides is important for the function of translation enhancers. We then designed All-U (5'-UUUUUUUUUU),

All-A (5'-AAAAAAAAAA), and Half-Eps (5'-UUAACGG-GAA) sequences as a model of the translation enhancer sequence. As shown in Figure 3D, increased binding of the 30S subunit to the All-U-CanSD mRNA (curve c) compared with the CanSD mRNA (curve a) was observed, and the All-A sequence (curve b) showed a minor effect on the binding of the 30S subunit. Kinetic parameters obtained from QCM analyses for mRNAs containing each enhancer sequence are summarized in Table 1 (runs 7–10). The value of $K_a = 23 \times 10^7 \text{ M}^{-1}$ for the All-U-CanSD mRNA was approximately four times higher than without enhancers ($K_a = 6.2 \times 10^7 \text{ M}^{-1}$ for the CanSD mRNA, run 2). Interestingly, the K_a value for the All-U-WeakSD mRNA (run 10) was considerably similar to that for the All-U-

Table 1. Binding Kinetic Parameters for the Interaction between the 30S Subunit or the S1-Depleted 30S (30S Δ S1) Subunit to mRNAs Containing Different SD and Enhancer Sequences and Translation Efficiencies of DHFR from Each mRNA Using the PURE System

| run | mRNA | ribosome | binding parameters ^a | | | translation efficiency of DHFR ^b |
|-----|----------------|-----------------|--|---|--|---|
| | | | k_{on} ($10^5 \text{ M}^{-1} \text{ s}^{-1}$) | k_{off} (10^{-3} s^{-1}) | K_{a} (10^7 M^{-1}) | |
| 1 | StrongSD | 30S | 1.8 \pm 0.42 | 2.1 \pm 0.30 | 8.6 \pm 2.3 | 1.4 |
| 2 | CanSD | 30S | 1.6 \pm 0.51 | 2.6 \pm 0.28 | 6.2 \pm 2.1 | 1 |
| 3 | WeakSD | 30S | 2.0 \pm 0.54 | 3.9 \pm 0.51 | 5.0 \pm 1.5 | 0.090 |
| 4 | Eps-StrongSD | 30S | 1.9 \pm 0.59 | 4.5 \pm 0.40 | 4.2 \pm 1.4 | 4.7 |
| 5 | Eps-CanSD | 30S | 1.9 \pm 1.2 | 4.4 \pm 0.60 | 4.3 \pm 2.8 | 4.6 |
| 6 | Eps-WeakSD | 30S | 5.7 \pm 1.6 | 8.2 \pm 0.13 | 6.9 \pm 2.0 | 0.12 |
| 7 | All-U-CanSD | 30S | 8.8 \pm 1.1 | 3.9 \pm 0.47 | 23 \pm 3.5 | 0.53 |
| 8 | Half-Eps-CanSD | 30S | 1.7 \pm 0.81 | 3.7 \pm 0.53 | 4.6 \pm 2.3 | 1.4 |
| 9 | All-A-CanSD | 30S | 2.2 \pm 0.4 | 1.9 \pm 0.22 | 12 \pm 2.5 | 1.2 |
| 10 | All-U-WeakSD | 30S | 7.4 \pm 1.3 | 3.4 \pm 0.58 | 22 \pm 5.3 | 0.14 |
| 11 | CanSD | 30S Δ S1 | 2.6 \pm 0.62 | 1.6 \pm 0.23 | 16 \pm 4.5 | 0.33 |
| 12 | Eps-CanSD | 30S Δ S1 | 2.4 \pm 0.62 | 1.2 \pm 0.21 | 20 \pm 6.2 | 0.52 |
| 13 | All-U-CanSD | 30S Δ S1 | 2.8 \pm 0.35 | 1.2 \pm 0.13 | 23 \pm 3.9 | 0.20 |
| 14 | Eps-A5-CanSD | 30S | 2.6 \pm 1.3 | 4.1 \pm 0.46 | 6.3 \pm 3.2 | 3.4 |
| 15 | Eps-A10-CanSD | 30S | 3.0 \pm 1.2 | 5.3 \pm 0.46 | 5.7 \pm 2.3 | 12 |
| 16 | Eps-A20-CanSD | 30S | 4.0 \pm 1.8 | 4.9 \pm 0.67 | 8.1 \pm 3.8 | 16 |
| 17 | Eps-R20-CanSD | 30S | 1.7 \pm 2.2 | 6.4 \pm 0.81 | 2.7 \pm 3.4 | 2.5 |

^a25 °C, 10 mM HEPES-KOH, pH 7.3, 100 mM NH₄Cl, 5 mM Mg(OAc)₂, 0.5 mM CaCl₂. ^bTranslation was performed with 1.2 μ g of mRNA and 30 μ L of PURE System for 1 h at 37 °C, and the translation efficiency of DHFR was evaluated from the UV absorbance at 340 nm (50 mM KH₂PO₄, pH 7.0, 50 mM DHF, 60 mM NADPH).

CanSD mRNA, independent of the SD sequence. These enhancements were derived from the remarkably increased k_{on} value. However, the All-U sequence lowered the translation efficiency of the CanSD mRNA (0.53 for the All-U-CanSD mRNA), whereas the All-U sequence slightly increased the translation efficiency for the All-U-WeakSD mRNA (0.14). Thus, the introduction of All-U (with 10 U bases) as the enhancer sequence increased the stability of the 30S/mRNA complex and thus decreased the translation in comparison with the Eps sequence (with 5 U bases). In contrast, the introduction of the All-A sequence as the enhancer sequence of the CanSD mRNA increased the stability of the 30S/mRNA complex ($K_{\text{a}} = 12 \times 10^7 \text{ M}^{-1}$) due to the decreased k_{off} value ($1.9 \times 10^{-3} \text{ s}^{-1}$). The translation efficiency (1.2) of the All-A-CanSD mRNA was almost the same as that of the CanSD mRNA (1). Conversely, the binding kinetics for the Half-Eps-CanSD mRNA showed moderate values of $k_{\text{on}} = 1.7 \times 10^8 \text{ M}^{-1} \text{ s}^{-1}$ and $k_{\text{off}} = 3.7 \times 10^{-3} \text{ s}^{-1}$, with a moderately higher translation efficiency of 1.4. Based on these results, the content of U nucleotides within the translation enhancer is responsible for the destabilization of the 30S/mRNA complex, but the excessive content U in the All-U sequence stabilizes the complex and may reduce the translation efficiency.

To confirm the interaction between the enhancer sequence and ribosomal protein S1, the binding kinetics of the S1-depleted 30S (30S Δ S1) subunit to each mRNA was studied. The 30S Δ S1 subunit can bind to the CanSD mRNA in the same manner, but the 30S Δ S1 subunit hardly bound to the mRNA without the CanSD sequence (Supporting Information Figure S6). The obtained kinetic parameters are summarized in Table 1 (runs 11–13). Similar kinetic parameters were obtained independent of the U nucleotide content of the enhancer region, with a high affinity of $K_{\text{a}} > 10^8 \text{ M}^{-1}$. The relative translation efficiencies of DHFR decreased by 0.33 for the CanSD mRNA, 0.52 for the Eps-CanSD mRNA, and 0.20 for the All-U-CanSD mRNA, compared with the intact 30S

subunit (runs 1, 4, and 7). Interestingly, although the affinity of the 30S Δ S1 subunit to the All-U-CanSD mRNA ($K_{\text{a}} = 23 \times 10^7 \text{ M}^{-1}$, run 13) is identical to the affinity of the intact 30S subunit to the All-U-CanSD mRNA ($K_{\text{a}} = 23 \times 10^7 \text{ M}^{-1}$, run 7), the k_{on} and k_{off} values are distinct. Instead, the k_{on} and k_{off} values are similar to those of the All-A-CanSD mRNA (run 9) and CanSD mRNA (run 1). These results indicate that the 30S Δ S1 subunit could only bind to the SD sequence without the enhancer sequence. Therefore, we conclude that the interaction between the S1 protein and the enhancer sequence is important to increase the translation efficiency.

Fluorescence Measurements of the Interactions between the 5'-End of mRNA and the 30S Subunit.

The structural information of the 30S/mRNA complex was investigated using fluorescently labeled mRNAs and 30S ribosome subunits. Here we employed a 5'-Cy3-labeled 30-mer RNA containing the CanSD, Eps-CanSD, and NonSD sequences (Figure 2C). When 100 nM of each Cy3-labeled mRNA was incubated with 100 nM of the 30S subunit, the fluorescence intensities increased (Figure 4A, curves d–f) compared with the mRNA by itself (curves a–c). Under these conditions, the 30S subunit is tightly bound to the mRNAs because the dissociation constant (K_{d}) is estimated to less than 10 nM (Table 1). The fluorescence increase indicates that the fluorescent group of Cy3 at the 5'-end of the mRNA is transferred to the hydrophobic environment of the 30S subunit. The intensity ratio of the fluorescence with or without the 30S subunit was highest when the Cy3-Eps-CanSD mRNA was employed (Figure 4B). The specific interaction between the Eps sequence and the S1 protein might therefore bring the 5'-end of the mRNA into the hydrophobic environment of the S1 protein. In contrast, the Cy3-CanSD mRNA containing no enhancer sequence showed a relatively small increase, which implied that its 5'-end did not bind tightly to the S1 protein and was more exposed to solvent. We also assayed fluorescence resonance energy transfer (FRET) experiments by introducing

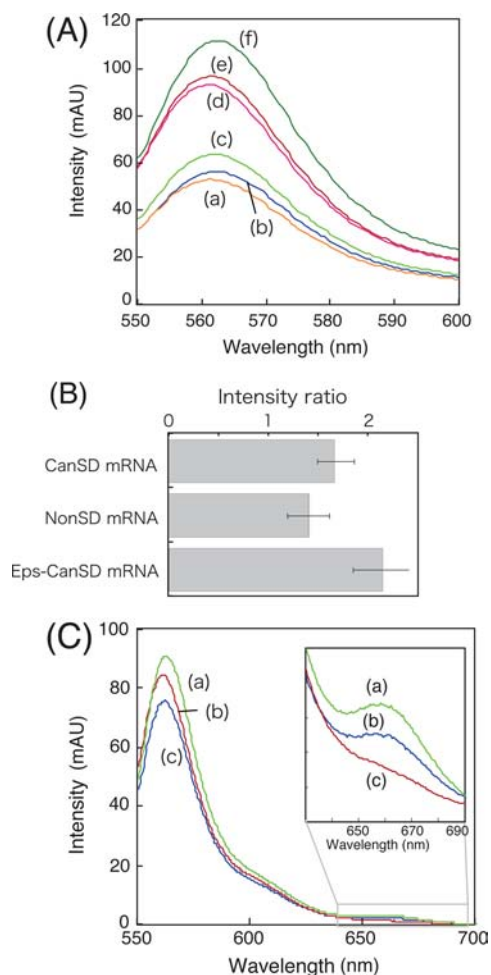


Figure 4. Fluorescent changes caused by bindings of Cy3-labeled mRNAs to the 30S subunit. (A) Overall fluorescence spectra of (a) the Cy3-Eps-CanSD mRNA, (b) the Cy3-CanSD mRNA, (c) the Cy3-NonSD mRNA, (d) the Cy3-NonSD mRNA + the 30S subunit, (e) the Cy3-CanSD mRNA + the 30S subunit, and (f) the Cys-Eps-CanSD mRNA + 30S subunit. (B) Intensity ratio of the fluorescence with or without the 30S subunit. (C) Overall fluorescence spectra of the solution containing both the Cy5-labeled 30S subunit and (a) the Cy3-Eps-CanSD mRNA, (b) the Cy3-CanSD mRNA, and (c) the Cy3-NonSD mRNA (10 mM HEPES-KOH pH 7.3, 100 mM NH_4Cl , 5 mM $\text{Mg}(\text{OAc})_2$, 0.5 mM CaCl_2 at room temperature).

Cy5 to a cysteine residue at the position of C292A of the S1 protein. The SH groups of S1 are located 6.8 Å from 3'-end of 16S rRNA.³¹ As shown in Figure 4C, the slight emission from Cy5 at 670 nm was detected when the Cy5-labeled 30S subunit was mixed with either the Cy3-Eps-CanSD mRNA or the Cy3-CanSD mRNA (Figure 4C, curves a and b, respectively). Conversely, the mixture of the Cy5-labeled 30S subunit and the Cy3-NonSD mRNA did not show any emission from Cy5 (curve c). Comparing the ratio of the intensity (Cy5/Cy3), the Eps-CanSD mRNA showed slightly higher fluorescence than the CanSD mRNA. These results also indicated that the 5'-end of the mRNA was proximally located on the S1 protein, and the topology of the Eps-CanSD mRNA bound on the 30S subunit was different from that of the CanSD mRNA.

Effect of Spacing Length on the Formation of the 30S/mRNA Complex and the Translation Efficiency. When mRNAs contain both the SD and enhancer sequences, the mRNAs would interact simultaneously or separately with

the anti-SD sequence and the S1 protein of the 30S subunit, respectively. It is possible that the distance between the SD and enhancer sequences of the mRNA affects the binding process and the translation efficiency. We introduced repeat adenine spacers (A5, A10, and A20) between the SD and enhancer (Eps) sequences (Figure 2A and C) and studied the binding kinetics of the 30S subunit using an mRNA-immobilized QCM. We also determined the translation efficiency using the cell-free expression PURE System. We expected that the adenine spacers did not interact with the 30S subunit and only altered the distance between the SD and Eps enhancer sequences. The results are summarized in Table 1 (runs 14–17). The binding kinetics (k_{on} , k_{off} and K_a) of the 30S subunit to the Eps-CanSD mRNA was hardly affected by the length of the adenine spacers (A5, A10, and A20) (runs 5, 14–16). On the contrary, the translation efficiency of DHFR increased by employing the Eps-A20-CanSD mRNA (16) and the Eps-A10-CanSD mRNA (12), in comparison with the Eps-CanSD mRNA (4.6). This enhancement was also observed in the GFP translation system using the Eps-A10-CanSD mRNA (Supporting Information, Figure S4, curves a and b) as well as the DHFR translation system (Supporting Information, Figure S4). We also confirmed that the adenine spacers further improved the translation efficiency in *E. coli* S30 cell extract, which is a much more conventional method than PURE system (Supporting Information of Figure S7). This result indicated that a long spacer between the Eps and SD sequences accelerated the initiation complex to move the translation (Steps 3 and 4 in Figure 1). However, when a random sequence spacer (Eps-R20-CanSD mRNA, Table 1, run 17) and a repeated uridine spacer (Eps-U10-CanSD mRNA, Supporting Information Figure S4) were employed, the translation efficiencies did not increase because of the interaction of the uridine spacers with the 30S subunit.

Real-Time Monitoring of the Translation Process on the QCM. We previously established a methodology to monitor the single turnover of protein synthesis using a 27 MHz QCM, as illustrated in Figure 5A and B.^{23,24} Using the mRNA encoding the fusion polypeptide of the streptavidin-binding peptide (SBP) tag, Protein D as a spacer, and the SecM arrest sequence, we could follow the binding of the 70S ribosome nascent chain complex (RNC), while the RNC was followed on the streptavidin-immobilized QCM by translating the SBP tag. Thus, we could follow the initial stage of the protein synthesis as a change in mass using the PURE System. This approach allowed us to evaluate the effect of the 5'-UTR region (the enhancer and SD sequences) on the translation of the SBP tag (Figure 5B). The time required for the translation of the SBP tag indicated the duration of forming the initiation complex and the following fast translation (the incorporation of the second aa-tRNA, Steps 3 and 4, Figure 1). By altering the trigger molecule for the translation start (mRNA or EF-Tu/GTP), we could evaluate the time required for the translation start (the time lag) and obtain the information of the rate-limiting step. Figure 5C shows typical time-courses of frequency decreases (mass increases) when the translation was started by the addition of mRNA. The extent of the lag time and the rate of production of the SBP tag (the slope of the frequency decrease) were dependent on the 5'-UTR sequence used. The results are summarized in Table 2. In the case of the mRNA trigger, both the Eps-CanSD mRNA (11.8 min) and the Eps-A10-CanSD mRNA (11.6 min) showed faster translation than that of the CanSD mRNA (15.2 min) (Figure 5C, curves

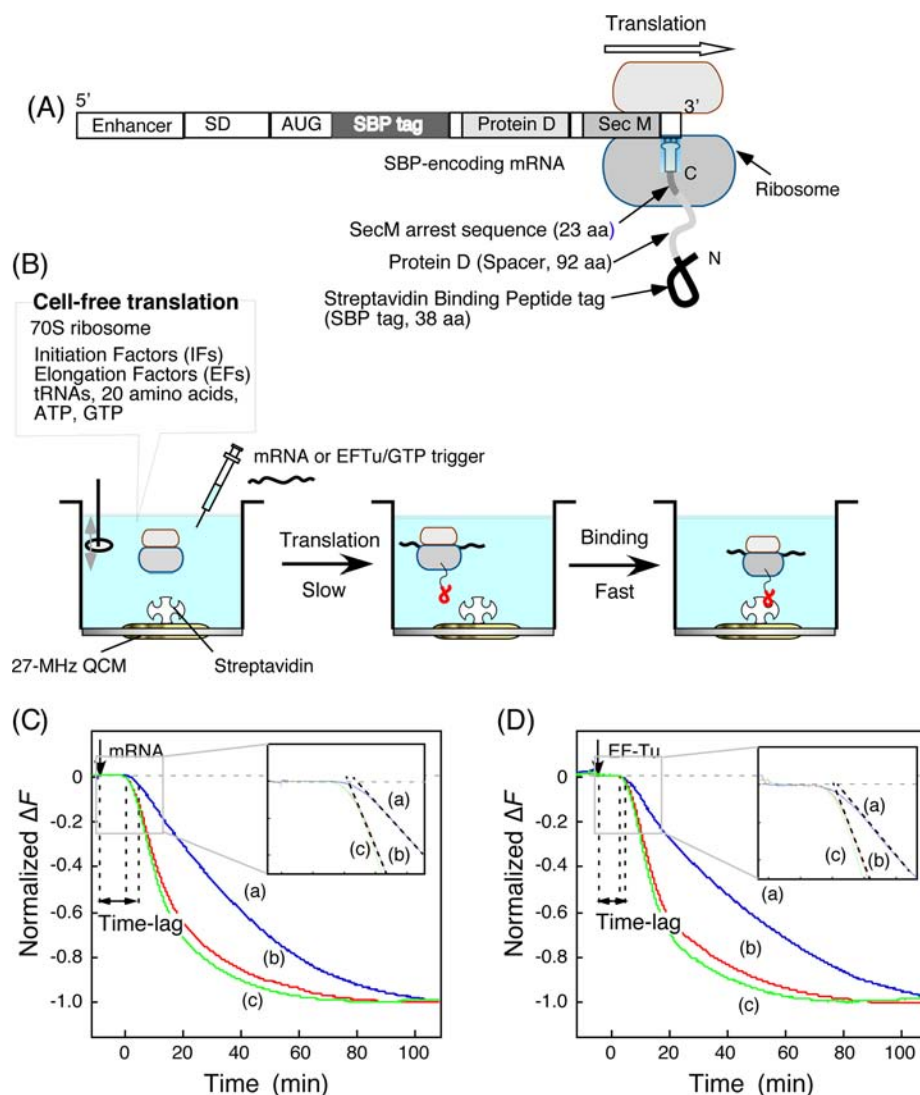


Figure 5. Schematic illustrations of (A) the 70S ribosome nascent chain complex (RNC) with the RNA encoding the fusion polypeptide containing the streptavidin-binding peptide (SBP) tag, Protein D as a spacer, and the SecM arrest sequence, and (B) trapping of the SBP tag of the RNC on the streptavidin-immobilized 27 MHz QCM, triggered by the addition of mRNA or EFTu/GTP using the PURE System. (C) Effect of different 5'-UTR sequences on the time lag between the addition of mRNA and the start of translation: (a) the CanSD mRNA, (b) the Eps-CanSD mRNA, and (c) the Eps-A10-CanSD mRNA. (D) Effect of the EF-Tu/GTP trigger on the time lag before the start of the translation in the presence of different 5'-UTR sequences: (a) the CanSD mRNA, (b) the Eps-CanSD mRNA, and (c) the Eps-A10-CanSD mRNA. The assays were conducted in the PURE System (a cell-free mixture with tRNAs from the MRE600 strain in 50 mM HEPES-KOH (pH 7.6) containing 100 mM potassium glutamate, 6 mM Mg(OAc)₂, 2 mM spermidine, and 1 mM dithiothreitol at 25 °C).

Table 2. Time Lags Obtained from the Translation of the SBP Tag on the QCM Using mRNAs with Different 5'-UTR Sequences, Triggered by mRNA or EFTu/GTP^a

| trigger | time lag/min | | |
|-----------|--------------|----------------|--------------------|
| | CanSD mRNA | Eps-CanSD mRNA | Eps-A10-CanSD mRNA |
| mRNA | 15.2 ± 0.22 | 11.8 ± 0.31 | 11.6 ± 0.47 |
| EF-Tu/GTP | 11.9 ± 0.27 | 10.2 ± 0.19 | 10.3 ± 0.20 |

^aThe assays were conducted in the cell-free mixture of the PURE System, with tRNAs from the MRE600 strain in 50 mM HEPES-KOH (pH 7.6) containing 100 mM potassium glutamate, 6 mM Mg(OAc)₂, 2 mM spermidine, and 2 mM dithiothreitol (DTT) at 25 °C.

b, c, and a, respectively, and Table 2). This result indicates that the Eps sequence enhances the translation of the SBP tag, independent of the A10 spacer. Using EF-Tu as a trigger,

ribosomes can form the initiation complex before the addition of EF-Tu/GTP (Figure 1). Thus, we could estimate the efficiency of the incorporation of the EF-Tu/aa-tRNA complex into the initiation complex from the frequency changes (Steps 3 and 4 of Figure 1). As shown in Figure 5D, the lag time of the Eps-CanSD mRNA (10.2 min) and the Eps-A10-CanSD mRNA (10.3 min) were similar to that of the CanSD mRNA (11.9 min). These results indicated that the Eps sequence facilitated the efficiency of the incorporation of the EF-Tu/aa-tRNA complex (Steps 3 and 4 of Figure 1) but not the binding of the mRNA to the 30S subunit (Step 1). The A10 spacer between the Eps and SD sequences had almost no effect on this step.

DISCUSSION

To translate the genetic information of the mRNAs, the bacterial ribosome must initially bind to a specific site of the 5'-UTR of the mRNA and then dissociate from the site to scan the

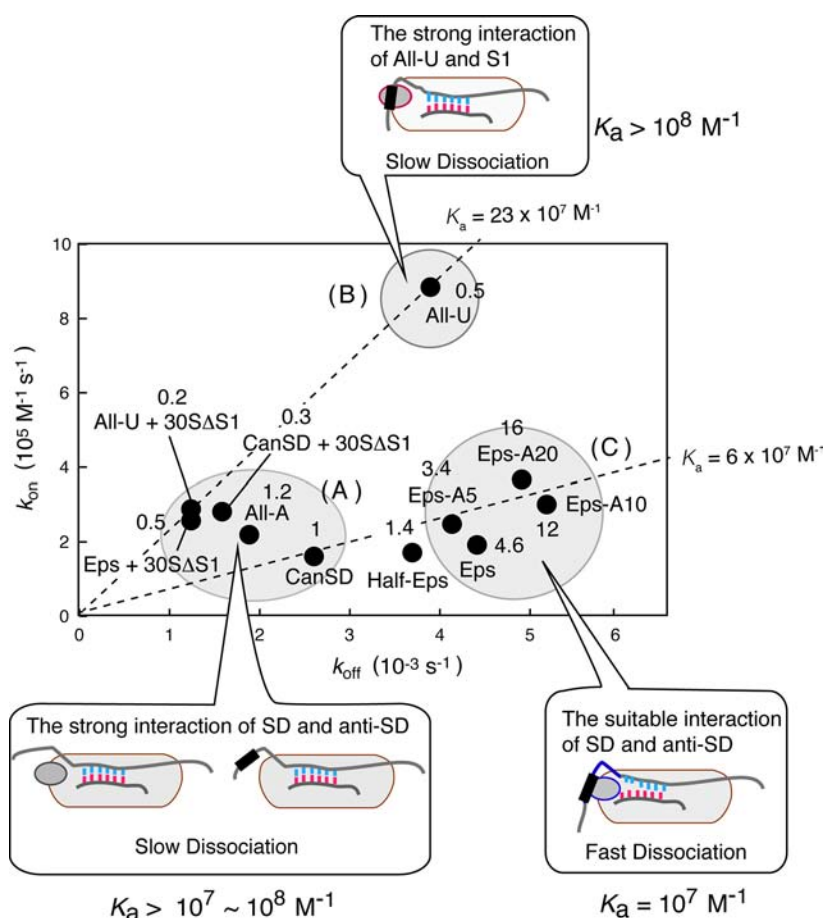


Figure 6. Correlations between the binding and dissociation rate constants (k_{on} and k_{off} , respectively) of the CanSD mRNA having different enhancer sequences to the 30S subunit and translation efficiencies of DHFR. The name of each mRNA is shown as just the enhancer sequence below the CanSD sequence. Numbers indicate the translation efficiency of DHFR for each mRNA. All plots can be grouped into three categories. (A) The group showing low k_{on} and k_{off} values, where a strong interaction between the SD and anti-SD sequences is predominant for the combination between the mRNA having no enhancer sequences (CanSD or All-A) and the 30S subunit, and for the combination between the mRNA having the Eps enhancer or the All-U sequence and the 30S Δ S1 subunit, resulting in low translation efficiencies (0.2–1.2). (B) The category showing the large k_{on} and k_{off} values, where a strong interaction between the All-U sequence and the S1 protein is predominant, resulting in a low translation efficiency (0.5). (C) The group showing low k_{on} and high k_{off} values, where the interaction between the SD and anti-SD is weakened by the spacer and the S1/Eps interaction, resulting in large translation efficiencies (3.4–16).

following genetic code on the mRNA in the 3'-direction during the peptide elongation phase. Therefore, the binding kinetics of the 30S subunit to the 5'-UTR (the 30S/mRNA complex formation, Step 1, and Steps 2–4, Figure 1) is key for achieving translation efficiency. In translation initiation in bacteria, ribosomal protein S1 plays a key role for the recognition of mRNA by ribosomes, in addition to the SD/anti-SD interaction. As reported previously, S1 has been shown to possess nucleic acid-helix-unwinding properties³² and to promote the initial binding of natural and structured mRNAs in *E. coli*.^{33–35} S1 is also an essential factor for efficient translation of mRNA with or without the SD sequence.^{33,36,37} The mechanism of interaction between the S1 protein and the enhancer sequence is still unclear because the S1 protein is not present in the crystal structural data of mRNA/ribosome complexes. Cryo-EM analysis suggested that the S1 protein interacts with both helix 45 of 16S rRNA as well as the immediate upstream region of the SD sequence on the mRNA.¹⁷ Furthermore, a previous study suggested that the binding of mRNA to the intact 30S subunit is dominated by the S1 protein,³⁷ whereas another study indicated that the 30S subunit simultaneously interacts with the SD and enhancer

sequences.¹⁰ Thus, a kinetic study of the binding of ribosomes to mRNA containing a translation enhancer can provide insight into the ribosomal dynamics related to translation efficiency during translation initiation.

Figure 6 shows the correlations between the binding and dissociation rate constants (k_{on} and k_{off} , respectively) of mRNAs to the 30S subunit and translation efficiencies of DHFR, depending on the 5'-UTR sequences. The content of U nucleotides of the enhancer sequence was responsible for the binding kinetics of 30S subunits to mRNAs. Based on the binding parameters of the mRNAs carrying the CanSD sequence, we could form three groups, A–C. Group A of mRNAs has no enhancer sequences (or All-A sequences), showing small k_{on} and k_{off} values with relatively large K_a values (10^7 – 10^8 M^{-1}). The binding between mRNAs having the Eps or All-U sequences and the S1-depleted 30S (30S Δ S1) subunit were also defined as Group A. Group B of mRNAs has All-U sequences, showing both large k_{on} and k_{off} values with high K_a values ($>10^8 \text{ M}^{-1}$). Group C of mRNAs has the Eps sequence as a general enhancer and shows small k_{on} and large k_{off} values with relatively small K_a values (10^7 M^{-1}). These unique differences in kinetic parameters can be determined by the

balance of two different interactions: the SD and anti-SD sequence interaction and the enhancer sequence and S1 protein interaction. The complementarity of the SD/anti-SD sequences is essential for stable formation of the 30S/mRNA complex and efficient translation. Furthermore, the S1 protein likely prefers the tandem U sequence because the S1 protein strongly binds to poly-U.^{29,30} The kinetic parameters indicate that the content of U at the enhancer region determine how much the enhancer/S1 interaction is dominant for the 30S/mRNA complex. Thus, the All-U sequence made a strong 30S/mRNA complex with a large k_{on} value, independent of the SD strength as previously reported²⁵ (see also Group B in Figure 6 and Table 1, runs 7 and 10). Similarly, the All-U sequence did not affect the binding to the 30S Δ S1 subunit due to the missing interaction between the S1 protein and the enhancer sequence (Group A). In contrast, when the mRNA has the Eps sequence, the K_a value becomes small (10^7 M^{-1}) because of the large k_{off} value (Group C). This indicates that the interaction between the Eps sequence and the S1 protein may destabilize the 30S/mRNA complex. This tendency is enhanced when A10 and A20 spacers are inserted between the Eps and CanSD sequences. Thus, long adenine spacers may destabilize the 30S/mRNA complex.

From correlations between binding kinetics and translation efficiency, we consider that the release of ribosomes from the initiation region of translation on mRNA is a key factor to determine the translation efficiency. In Group A, both the combination between mRNAs with no enhancer sequences (or with the All-A sequence) and the intact 30S subunit as well as the combination between mRNAs with the strong All-U or Eps enhancer sequences and the 30S Δ S1 subunit showed the relatively large K_a values (10^7 – 10^8 M^{-1}) with small k_{on} and k_{off} values and low translation efficiencies (0.2–1). This result can be explained by the strong interaction between the SD and anti-SD sequences observed when the 5'-UTR sequence downstream of the SD sequence could not interact with the 30S subunit. As a result, the initiation complex was stabilized, and the following translation was disturbed. In the case of Group B, the mRNA with the All-U sequence at the 5'-UTR showed a large $K_a = 23 \times 10^7 \text{ M}^{-1}$ with large k_{on} and k_{off} values and a low translation efficiency. This result can be explained by the strong interaction of the All-U sequence with the S1 protein in addition to the interaction between the SD/anti-SD sequences, stabilizing the initiation complex and disturb the subsequent translation step. Conversely, mRNAs of Group C with the general enhancer sequence of Eps showed a weak initiation complex, with $K_a = 10^7 \text{ M}^{-1}$, small k_{on} and large k_{off} values, and high translation efficiencies. The translation efficiencies increased to 12 and 16 when the A10 and A20 adenine spacers, respectively, were introduced between the Eps and CanSD sequences because a suitable interaction between the Eps sequence and the S1 protein may reduce the SD/anti-SD interaction, especially when the long A20 spacer was introduced. Thus, the k_{off} value increased (proceeding to Steps 2–4, Figure 1), and the translation efficiency increased.

Recent structural studies indicated that the movement of the 30S/mRNA complex is involved in the transformation of the initiation complex into the postinitiation complex (peptide-elongation complex) and that the second aa-tRNA binds to the postinitiation complex rather than the initiation complex.¹⁹ Single-molecule analyses also revealed that the SD/anti-SD interaction was weakened during the accommodation of the second aa-tRNA.³⁸ Therefore, our results of the single-turnover

translation triggered by EF-Tu implied that the translation enhancer facilitated the dissociation of the SD/anti-SD interaction before the next aa-tRNA accommodation (see Step 3 in Figure 1). Because the SD/anti-SD interaction moves dynamically through the process of the formation of the initiation complex, the adenine spacer insert between the enhancer and SD sequences may help its dynamics to improve the speed of its formation. However, the kinetics of the 30S/mRNA complex and the initiation complex formation are not dependent on the presence of the translation enhancer on mRNA (unpublished data).

The processive mode of ribosomes is often regulated by the mRNA sequence itself. Ribosomes decelerate the translation rate during decoding of rare codons or SD like sequences.^{24,39–41} It is also possible that the secondary structure of mRNA causes a stall of the translating ribosome.^{42,43} Polyadenine sequences, such as the 5'-UTR sequence, facilitate ribosome scanning to start translation, which is considered the noncanonical translation initiation such as the translation of leaderless mRNAs. Passive interaction of ribosomes to mRNA is a common mechanism to tune the translation manner. The translation initiation is the rate-limiting process in the translation cycle. Therefore, it is critical to increase the efficiency of the translation by promoting the liberation of the ribosome from translation initiation.

CONCLUSION

Our results show that the combination of the two interactions of the SD/anti-SD and enhancer/S1 can be responsible for the transition state from the initiation step to the elongation step by a negative allosteric effect. In nature, general enhancer sequences, including the Eps sequence, have tandem repeats of U and A nucleotides. Based on the results reported, U nucleotides promote the interaction between the S1 protein and mRNA, but A nucleotides do not promote this interaction. Translation enhancers regulate the release of the ribosome from the initiation region of translation on mRNA by tuning kinetic parameters, especially the k_{off} value. There are several enhancers, such as the Eps sequence, on phage genes. These gene expressions should therefore be extraordinary in *E. coli*. Therefore, endogenous gene expression may be deliberately maintained at a relative low level to suppress the liberation of ribosomes from translation initiation.

MATERIALS AND METHODS

Preparation of Ribosomes and Translational Factors. *E. coli* 70S ribosomes and 30S ribosomal subunits were isolated and purified from *E. coli* A19 cells as described previously.^{44,45} The S1-depleted 30S (30S Δ S1) subunit was prepared according to a previous paper.⁴⁵ All translational factors for the PURE System were purified as described previously.^{26,27}

Design and Preparation of mRNAs. Biotinylated mRNAs were designed for the immobilization on 27 MHz QCMs (Figure 2A), and mRNAs were designed for protein (DHFR or GFP) synthesis (Figure 2B). Each mRNA contained SD sequences (CanSD: AAGGAGGCA, StrongSD: UAAGGAGGUG, or WeakSD: ACAGGCGCCA, where the double-underlines indicate the complementary sequence to the anti-SD sequence of the 30S subunit) and/or the translation enhancer (Eps: UUAACUUUAA, Half-Eps: UUAACGGGAA, All-U: UUUUUUUUUU, All-A: AAAAAAAAAA, where the underlines indicate pyrimidine nucleotides showing the strong interaction to S1 protein of the 30S subunit), and/or the adenine spacer of A5, A10, and A20. The complete sequence of each mRNA is described in the Supporting Information (Figure S1). For *in vitro* translation

experiments, the gene of DHFR was connected to the T7 promoter region, and each cDNA was synthesized by PCR from the 5'-UTR of the mRNA. These PCR products were phosphorylated by T4 kinase, digested by *Pst*I, and inserted into pUC18 digested by *Pst*I and *Sma*I. The obtained plasmids were digested by *Pst*I, and each mRNA was transcribed by T7 RNA polymerase. All mRNAs were purified and stored at $-80\text{ }^{\circ}\text{C}$ before use.

Evaluation for Translation Efficiency Using the PURE System. The PURE System^{26,27} was used to determine the translation efficiency of the mRNAs of DHFR depending on the 5'-UTR sequence. The protein synthesis reactions for DHFR were started by the addition of 1.2 μg of each mRNA to 30 μL of the PURE System reaction mixture, followed by incubation for 1 h at $37\text{ }^{\circ}\text{C}$. The reactions were stopped by cooling on ice and applied four times volume of 50 mM KH_2PO_4 (pH 7.0). To measure the amount of DHFR,⁴⁶ 10 μL of solution was added to 190 μL of assay solution (50 mM KH_2PO_4 pH 7.0, 50 μM DHF, 60 μM NADPH), and the UV absorbance at 340 nm of each solution was measured every 30 s. The amount of DHFR translation was evaluated as the initial rate of the decrease in the absorbance over several seconds.

QCM Experiments To Obtain Binding Kinetic Parameters of 30S Subunit to mRNA. Calibrations for the 27-MHz QCM experiments in aqueous solutions were performed as reported previously.²² Briefly, NeutrAvidin (Pierce, Waltham, USA) was immobilized on a 27 MHz QCM plate. The QCM cell was connected into AFFINIX Q4 (Initium, Tokyo, Japan) with 500 μL of the measurement buffer (10 mM HEPES-KOH pH 7.3, 100 mM NH_4Cl , 5 mM $\text{Mg}(\text{OAc})_2$, 0.5 mM CaCl_2) at $25\text{ }^{\circ}\text{C}$. The biotinylated mRNA was injected into the QCM cell, and 1 μL of 10 mM biotin solution was added to stop the binding of the biotinylated mRNA when the frequency decrease reached -27 Hz . The solution in the QCM cell was rinsed several times with pure water and then filled with 500 μL of the measurement buffer. Ribosome 30S subunits were added several times into the QCM cell to obtain the binding constant and the maximum binding amount as reported previously.²² To determine the kinetic parameters (k_{on} and k_{off}), time-courses of frequency changes for several different concentrations of 30S subunit were fitted with a single exponential equation to obtain the relaxation time (τ) of the ribosome binding, as described previously.^{22–24} The noise level of the 27 MHz QCM was $\pm 1\text{ Hz}$ in buffer solutions at $25\text{ }^{\circ}\text{C}$, and the standard deviation of the frequency was $\pm 2\text{ Hz}$ for 1 h in buffer solutions at $25\text{ }^{\circ}\text{C}$. A sensitivity of 0.19 ng/cm² per -1 Hz is sufficiently large to sense the binding of ribosomes.

Fluorescence Analysis. Each Cy3-labeled RNA was prepared by solid-phase synthesis using phosphoramidite monomers purchased from Nihon Techno Service (Tokyo, Japan). All RNAs were purified by HPLC and confirmed by matrix-assisted laser desorption ionization time-of-flight mass spectrometry (MALDI TOF-MS). S1 single point mutant proteins, S1 C249A and S1 C369A, were expressed in *E. coli* BL21 using plasmids encoding His-tagged S1 mutant proteins. All proteins were purified under denaturing conditions (using urea) and then modified with Cy5 maleimide (GE Healthcare) in the presence of guanidine HCl. Renatured S1 was incubated with S1-free 30S to obtain Cy5–30S, as described.³¹

The Cy3-labeled mRNA (100 nM) was incubated for 15 min at room temperature with 100 nM 30S subunit or 100 nM Cy5-labeled 30S subunit in the measurement buffer together with 5% SlowFade Antifade kit (Invitrogen). The reference experiment with only the Cy3-labeled mRNA was conducted in the presence of 7 M Urea. Fluorescence spectra were acquired after excitation at 532 nm.

Single-Turnover Translation Measurements on QCMs. The 5'-UTR sequence was connected to a fusion protein consisting of SBP tag, Protein D as a spacer, and the SecM arrest sequence, as shown in Figure SA.²³ Each mRNA was transcribed from each constructed DNA and used for translation in the QCM cell, with or without EF-Tu, as described previously.²³

■ ASSOCIATED CONTENT

■ Supporting Information

The full sequence of mRNAs used in this study (Figure S1), SDS-PAGE analysis for the reactants of PURE system (Figure S2), isothermal titration curve for 30S binding to mRNAs (Figure S3), fluorescence spectra showing the translation efficiency of DFP proteins from different mRNAs (Figure S4), relative translation efficiencies of GFP and DHFR from different mRNAs (Figure S5), QCM data of the 30S Δ S1 subunit bindings to mRNAs (Figure S6), and a translation assay in *E. coli* cell-free extract (Figure S7). This material is available free of charge via the Internet at <http://pubs.acs.org>.

■ AUTHOR INFORMATION

Corresponding Author

yokahata@yz.yamagata-u.ac.jp; shtakaha@center.konan-u.ac.jp

Notes

The authors declare no competing financial interest.

■ ACKNOWLEDGMENTS

We thank Professor Sekine and Dr. Tsunoda of Tokyo Institute of Technology for help with labeled RNA synthesis. We also acknowledge Mr. Sugahara for help with experiments. This work was supported by the Ministry of Education, Culture, Sports, Science and Technology of Japan, Grant-in-Aid for Scientific Research (22225005 to Y.O. and 22750147 to S.T.) and the Japan Science and Technology Agency (JST), Technology Development Program for Advanced Measurement and Analysis (to Y.O.).

■ REFERENCES

- (1) Laursen, B. S.; Sorensen, H. P.; Mortensen, K. K.; Sperling-Petersen, H. U. *Microbiol. Mol. Biol. Rev.* **2005**, *69*, 101–123.
- (2) Kozak, M. *Gene* **1999**, *234*, 187–208.
- (3) Shine, J.; Dalgarno, L. *Proc. Natl. Acad. Sci. U.S.A.* **1974**, *71*, 1342.
- (4) McCarthy, J.; Schairer, H. U.; Sebald, W. *EMBO J.* **1985**, *4*, 519.
- (5) Olins, P. O.; Devine, C. S.; Rangwala, S. H.; Kavka, K. S. *Gene* **1988**, *73*, 227–235.
- (6) Gallie, D.; Kado, C. *Proc. Natl. Acad. Sci. U.S.A.* **1989**, *86*, 129–132.
- (7) Hartz, D.; McPheeters, D. S.; Gold, L. *J. Mol. Biol.* **1991**, *218*, 83–97.
- (8) Loechel, S.; Inamine, J. M.; Hu, P.-c. *Nucleic Acids Res.* **1991**, *19*, 6905–6911.
- (9) Boni, I. V.; Artamonova, V. S.; Tzareva, N. V.; Dreyfus, M. *EMBO J.* **2001**, *20*, 4222–4232.
- (10) Komarova, A. V.; Tchufistova, L. S.; Supina, E. V.; Boni, I. V. *RNA* **2002**, *8*, 1137–1147.
- (11) Balakin, A.; Bogdanova, S.; Skripkin, E. *Biochem. Int.* **1992**, *27*, 117.
- (12) Suryanarayana, T.; Subramanian, A. *J. Mol. Biol.* **1979**, *127*, 41–54.
- (13) Boni, I. V.; Musychenko, M. L.; Tzareva, N. V. *Nucleic Acids Res.* **1991**, *19*, 155–162.
- (14) Zhang, J.; Deutscher, M. P. *Proc. Natl. Acad. Sci. U.S.A.* **1992**, *89*, 2605–2609.
- (15) Tzareva, N.; Makhno, V.; Boni, I. *FEBS Lett.* **1994**, *337*, 189–194.
- (16) Ringquist, S.; Jones, T.; Snyder, E. E.; Gibson, T.; Boni, I.; Gold, L. *Biochemistry* **1995**, *34*, 3640–3648.
- (17) Sengupta, J.; Agrawal, R. K.; Frank, J. *Proc. Natl. Acad. Sci. U.S.A.* **2001**, *98*, 11991.
- (18) Zavialov, A. V.; Hauryliuk, V. V.; Ehrenberg, M. *Mol. Cell* **2005**, *18*, 675–686.

- (19) Yusupova, G.; Jenner, L.; Rees, B.; Moras, D.; Yusupov, M. *Nature* **2006**, *444*, 391–394.
- (20) Takahashi, S.; Matsuno, H.; Furusawa, H.; Okahata, Y. *Anal. Biochem.* **2007**, *361*, 210–217.
- (21) Takahashi, S.; Matsuno, H.; Furusawa, H.; Okahata, Y. *J. Biol. Chem.* **2008**, *283*, 15023–15030.
- (22) Takahashi, S.; Akita, R.; Matsuno, H.; Furusawa, H.; Shimizu, Y.; Ueda, T.; Okahata, Y. *ChemBioChem* **2008**, *9*, 870–873.
- (23) Takahashi, S.; Iida, M.; Furusawa, H.; Shimizu, Y.; Ueda, T.; Okahata, Y. *J. Am. Chem. Soc.* **2009**, *131*, 9326–9332.
- (24) Takahashi, S.; Tsuji, K.; Ueda, T.; Okahata, Y. *J. Am. Chem. Soc.* **2012**, *134*, 6793–6800.
- (25) Studer, S. M.; Joseph, S. *Mol. Cell* **2006**, *22*, 105–115.
- (26) Shimizu, Y.; Inoue, A.; Tomari, Y.; Suzuki, T.; Yokogawa, T.; Nishikawa, K.; Ueda, T. *Nat. Biotechnol.* **2001**, *19*, 751–755.
- (27) Shimizu, Y.; Kanamori, T.; Ueda, T. *Methods* **2005**, *36*, 299–304.
- (28) Olins, P. O.; Rangwala, S. H. *J. Biol. Chem.* **1989**, *264*, 16973–16976.
- (29) Suryanarayana, T.; Subramanian, A. R. *Biochemistry* **1984**, *23*, 1047–1051.
- (30) Subramanian, A. R. *Trends Biochem. Sci.* **1984**, *9*, 491–494.
- (31) Odom, O. W.; Dabbs, E. R.; Dionne, C.; Müller, M.; Hardesty, B. *Eur. J. Biochem.* **1984**, *142*, 261–267.
- (32) Kolb, A.; Hermoso, J. M.; Thomas, J. O.; Szer, W. *Proc. Natl. Acad. Sci. U.S.A.* **1977**, *74*, 2379–2383.
- (33) Sorensen, M. A.; Fricke, J.; Pedersen, S. J. *Mol. Biol.* **1998**, *280*, 561–569.
- (34) de Smit, M. H.; van Duin, J. *J. Mol. Biol.* **1994**, *235*, 173.
- (35) Boni, I. V.; Isaeva, D. M.; Musychenko, M. L.; Tzareva, N. V. *Nucleic Acids Res.* **1991**, *19*, 155–162.
- (36) Melancon, P.; Leclerc, D.; Destroismaisons, N.; Brakier-Gingras, L. *Biochemistry* **1990**, *29*, 3402–3407.
- (37) Tedin, K.; Resch, A.; Bläsi, U. *Mol. Microbiol.* **1997**, *25*, 189–199.
- (38) Uemura, S.; Dorywalska, M.; Lee, T. H.; Kim, H. D.; Puglisi, J. D.; Chu, S. *Nature* **2007**, *446*, 454–457.
- (39) Li, G.-W.; Oh, E.; Weissman, J. S. *Nature* **2012**, *484*, 538–541.
- (40) Wen, J. D.; Lancaster, L.; Hodges, C.; Zeri, A. C.; Yoshimura, S. H.; Noller, H. F.; Bustamante, C.; Tinoco, I. *Nature* **2008**, *452*, 598–603.
- (41) Endoh, T.; Kawasaki, Y.; Sugimoto, N. *Anal. Chem.* **2011**, *84*, 857–861.
- (42) Watts, J. M.; Dang, K. K.; Gorelick, R. J.; Leonard, C. W.; Bess, J. W., Jr; Swanstrom, R.; Burch, C. L.; Weeks, K. M. *Nature* **2009**, *460*, 711–716.
- (43) Endoh, T.; Kawasaki, Y.; Sugimoto, N. *Angew. Chem., Int. Ed.* **2013**, *125*, 5632–5636.
- (44) Ohashi, H.; Shimizu, Y.; Ying, B. W.; Ueda, T. *Biochem. Biophys. Res. Commun.* **2007**, *352*, 270–276.
- (45) Udagawa, T.; Shimizu, Y.; Ueda, T. *J. Biol. Chem.* **2004**, *279*, 8539–8546.
- (46) Qi, H.; Shimizu, Y.; Ueda, T. *J. Mol. Biol.* **2007**, *368*, 845–852.